Journal Pre-proofs

Article

Global wood anatomical perspective on the onset of the Late Antique Little Ice Age (LALIA) in the mid-6th century CE

Ulf Büntgen, Alan Crivellaro, Dominique Arseneault, Mike Baillie, David Barclay, Mauro Bernabei, Jarno Bontadi, Gretel Boswijk, David Brown, Duncan A. Christie, Olga V. Churakova(Sidorova), Edward R. Cook, Rosanne D'Arrigo, Nicole Davi, Jan Esper, Patrick Fonti, Ciara Greaves, Rashit M. Hantemirov, Malcolm K. Hughes, Alexander V. Kirdyanov, Paul J. Krusic, Carlos Le Quesne, Fredrik C. Ljungqvist, Michael McCormick, Vladimir S. Myglan, Kurt Nicolussi, Clive Oppenheimer, Jonathan Palmer, Chun Qin, Frederick Reinig, Matthew Salzer, Markus Stoffel, Max Torbenson, Mirek Trnka, Ricardo Villalba, Nick Wiesenberg, Greg Wiles, Bao Yang, Alma Piermattei

PII: S2095-9273(22)00479-0
DOI: https://doi.org/10.1016/j.scib.2022.10.019
Reference: SCIB 1911

To appear in: *Science Bulletin*

Received Date: 23 June 2022
Revised Date: 23 August 2022
Accepted Date: 24 August 2022

Please cite this article as: U. Büntgen, A. Crivellaro, D. Arseneault, M. Baillie, D. Barclay, M. Bernabei, J. Bontadi, G. Boswijk, D. Brown, D.A. Christie, O.V. Churakova,(Sidorova) E.R. Cook, R. D'Arrigo, N. Davi, J. Esper, P. Fonti, C. Greaves, R.M. Hantemirov, M.K. Hughes, A.V. Kirdyanov, P.J. Krusic, C. Le Quesne, F.C. Ljungqvist, M. McCormick, V.S. Myglan, K. Nicolussi, C. Oppenheimer, J. Palmer, C. Qin, F. Reinig, M. Salzer, M. Stoffel, M. Torbenson, M. Trnka, R. Villalba, N. Wiesenberg, G. Wiles, B. Yang, A. Piermattei, Global wood anatomical perspective on the onset of the Late Antique Little Ice Age (LALIA) in the mid-6th century CE, *Science Bulletin* (2022), doi: https://doi.org/10.1016/j.scib.2022.10.019

Global wood anatomical perspective on the onset of the Late Antique Little Ice Age (LALIA) in the mid-6th century CE

Ulf Büntgen [1,2,3,4,*], Alan Crivellaro [1,5], Dominique Arseneault [6], Mike Baillie [7], David Barclay [8], Mauro Bernabei [9], Jarno Bontadi [9], Gretel Boswijk [10], David Brown [7], Duncan A. Christie [11,12,13], Olga V. Churakova (Sidorova) [14], Edward R. Cook [15], Rosanne D'Arrigo [15], Nicole Davi [15,16], Jan Esper [3,17], Patrick Fonti [2], Ciara Greaves [1], Rashit M. Hantemirov [18,19], Malcolm K. Hughes [20], Alexander V. Kirdyanov [14,21], Paul J. Krusic [1,22], Carlos Le Quesne [11], Fredrik C. Ljungqvist [23,24,25], Michael McCormick [26], Vladimir S. Myglan [27], Kurt Nicolussi [28], Clive Oppenheimer [1], Jonathan Palmer [29], Chun Qin [30], Frederick Reinig [17], Matthew Salzer [20], Markus Stoffel [31,32,33], Max Torbenson [17], Mirek Trnka [3], Ricardo Villalba [34], Nick Wiesenberg [35], Greg Wiles [35], Bao Yang [30,36], Alma Piermattei [1]

[1]*Department of Geography, University of Cambridge, Cambridge CB2 3EN, UK.*

[2]*Swiss Federal Research Institute (WSL), 8903 Birmensdorf, Switzerland.*

[3]*Global Change Research Centre (CzechGlobe), Brno 60300, Czech Republic.*

[4]*Department of Geography, Faculty of Science, Masaryk University, Brno 61300, Czech Republic.*

[5]*Forest Biometrics Laboratory, Faculty of Forestry, "Stefan cel Mare" University of Suceava, Suceava 720229, Romania.*

[6]*Department of Biology, Chemistry and Geography, University of Quebec in Rimouski, Rimouski Qc. G5L 3A1, Canada.*

[7]*Archaeology & Palaeoecology, School of Natural and Built Environment, Queen's University Belfast, Belfast BT7 1NN, UK.*

[8]*Department of Geology, State University of New York at Cortland, Cortland NY 13045, USA.*

[9]*CNR-IBE, Institute of BioEconomy, National Research Council, Trento 38121, Italy.*

[10]School of Environment, The University of Auckland, Auckland 1010, New Zealand.

[11]Laboratorio de Dendrocronología y Cambio Global, Universidad Austral de Chile, Valdivia 509000, Chile.

[12]Center for Climate and Resilience Research (CR), Santiago 8370449, Chile.

[13]Cape Horn International Center (CHIC), Punta Arenas 6200000, Chile.

[14]Institute of Ecology and Geography, Siberian Federal University, Krasnoyarsk 660041, Russia.

[15]Tree-Ring Laboratory, Lamont-Doherty Earth Observatory, Columbia University, Palisades NY 10964, USA.

[16]Department of Environmental Science, William Paterson University, Wayne NJ 07470, USA.

[17]Department of Geography, Johannes Gutenberg University, Mainz 55099, Germany.

[18]Institute of Plant and Animal Ecology, Ural Branch, Russian Academy of Sciences, Yekaterinburg 620144, Russia.

[19]Ural Institute of Humanities, Ural Federal University, Yekaterinburg 620002, Russia.

[20]Laboratory of Tree-Ring Research, University of Arizona, Tucson AZ 85721, USA.

[21]Sukachev Institute of Forest SB RAS, Krasnoyarsk 660036, Russia.

[22]Department of Physical Geography, Bolin Centre for Climate Research, Stockholm University, Stockholm 10691, Sweden.

[23]Department of History, Stockholm University, Stockholm 10691, Sweden.

[24]Bolin Centre for Climate Research, Stockholm University, Stockholm 10691, Sweden.

[25]Swedish Collegium for Advanced Study, Uppsala 75238, Sweden.

[26]Initiative for the Science of the Human Past, Department of History-Max Planck Harvard Research Center for the Archaeoscience of the Ancient Mediterranean, Harvard University, Cambridge MA 02138, USA.

[27]Institute of Humanities, Siberian Federal University, Krasnoyarsk 660041, Russia.

[28]Department of Geography, University of Innsbruck, Innsbruck 6020, Austria.

[29]The University of New South Wales, Sydney NSW 2052, Australia.

[30]*Key Laboratory of Desert and Desertification, Northwest Institute of Eco-Environment and Resources, Chinese Academy of Sciences, Lanzhou 730000, China.*

[31]*Change Impacts and Risks in the Anthropocene (C-CIA), Institute for Environmental Sciences, University of Geneva, Geneva 1205, Switzerland.*

[32]*Department of Earth Sciences, University of Geneva, Geneva 1205, Switzerland.*

[33]*Department F.-A. Forel for Environmental and Aquatic Sciences, University of Geneva, Geneva 1205, Switzerland.*

[34]*National Scientific and Technical Research Council, Instituto Argentino de Nivología, Glaciología y Ciencias Ambientales, Mendoza CP 5500, Argentina.*

[35]*Department of Earth Sciences, the College of Wooster, Wooster OH 44691, USA.*

[36] *Center for Excellence in Tibetan Plateau Earth Sciences, Chinese Academy of Sciences, Beijing 100101, China.*

*Corresponding author: ulf.buentgen@geog.cam.ac.uk

Received 2022-06-23，revised 2022-08-23，accepted 2022-08-24

Abstract

Linked to major volcanic eruptions around 536 and 540 CE, the onset of the Late Antique Little Ice Age has been described as the coldest period of the past two millennia. The exact timing and spatial extent of this exceptional cold phase are, however, still under debate because of the limited resolution and geographical distribution of the available proxy archives. Here, we present 106 wood anatomical thin sections from 23 forest sites and 20 tree species in both hemispheres to search for cell-level fingerprints of ephemeral summer cooling between 530 and 550 CE. After cross-dating and double-staining, we identified 89 Blue Rings (lack of cell wall lignification), nine Frost Rings (cell deformation and collapse), and 93 Light Rings (reduced cell wall thickening) in the Northern Hemisphere. Our network reveals evidence for the strongest temperature depression between mid-July and early-August 536 CE across North America and Eurasia, whereas more localised cold spells

occurred in the summers of 532, 540–43, and 548 CE. The lack of anatomical signatures in the austral trees suggests limited incursion of stratospheric volcanic aerosol into the Southern Hemisphere extra-tropics, that any forcing was mitigated by atmosphere-ocean dynamical responses and/or concentrated outside the growing season, or a combination of factors. Our findings demonstrate the advantage of wood anatomical investigations over traditional dendrochronological measurements, provide a benchmark for Earth system models, support cross-disciplinary studies into the entanglements of climate and history, and question the relevance of global climate averages.

Keywords

Blue Rings, climate extremes, dendrochronology, Late Antiquity, tree rings, volcanic eruptions.

1. Introduction

With the brief title “Mystery cloud of AD 536”, Stothers [1] triggered an enduring quest to understand the relationships between volcanism, climate, and history in the mid-6th century CE. In his pioneering work, the astronomer and planetary scientist drew on observations of solar dimming recorded by Byzantine writers to infer the presence of stratospheric volcanic aerosol. His interpretations were substantiated by subsequent studies of Greenland ice cores, which confirmed the volcanic origin of the “mystery cloud” and further revealed that it was succeeded, just four years later, by another stratospheric sulfate aerosol veil [2]. The later event in circa 540 CE has been linked to an eruption of Ilopango in El Salvador, Central America, consistent with the tropical location suggested by a pattern of sulfur deposition in bipolar ice cores [3], though this attribution remains disputed [4]. Ice core evidence points to a Northern Hemisphere extra-tropical volcano as source of the circa 536 CE dust veil [2].

The two putative eruptions in 536 and 540 CE most likely caused the strongest summer cooling over much of the Northern Hemisphere in the past two millennia [5–7], as revealed by several tree ring-based growing season temperature reconstructions and corroborated by coupled aerosol-climate

model simulations [8]. With a mean and median of -1.54 and -1.54 °C and a range of -0.58 to -3.56 °C with respect to the 1961–90 mean (Fig. 1a, b), a community-driven ensemble of 15 state-of-the-art dendroclimatological reconstructions assigns 536 CE to the coldest boreal summer of the Common Era [7]. It defines the onset of the so-called Late Antique Little Ice Age (LALIA) (Fig. 1c, d), which possibly lasted up to the mid-7th century [5], at least in central Europe and inner Eurasia. Independent lines of archaeological, climatological, environmental, and historical evidence have substantiated the LALIA concept and brought refinements to its chronology [5–18]. The cluster of exceptionally cold summers at the onset of the LALIA in the 530s and 540s coincides with harvest failures, famines and pestilence spanning at least Mesoamerica and northern North America, Europe including the British Isles and Scandinavia, the Mediterranean, inner Eurasia, and large parts of China [1,2,5,19–24].

Among the historical events that may relate to the LALIA are [5]: (1) the outbreak of the Justinianic Plague between 541 and 543 CE across the Later Roman (Byzantine) Empire. (2) The demise of the Northern Wei Dynasty in the 530s CE, which was followed by a series of short-lived Chinese dynasties. (3) The replacement of the Rouran as the dominant steppe power across inner Eurasia by the Türks in the early-550s CE, who went on to defeat the Avars and the Hephthalite Huns in the following decade, took control of the trading towns of the Sogdians, and initiated exchanges with the Persian Empire that brought central Asian silk to Persia. (4) The arrival of at least two ethnic groups north of the Black Sea and Pannonia, which engaged in diplomatic relations but also military conflict with the Romans, possibly playing a role in the Lombards' invasion of Italy in 568 CE (see [5] for further details). It should be further noted that much of Scandinavia and the Baltic countries witnessed an unprecedented shift in settlement locations and a population decline of up to 50% in the mid-6th century [25]. It has also been argued that this period coincides with a demographic collapse of the Maya civilisation in Mesoamerica in the early 540s associated with the Tierra Blanca Joven eruption of Ilopango volcano in El Salvador [3]. We do not suggest these historical episodes are a direct consequence of the LALIA but do argue that it should be considered

as an environmental factor embroiled with other chance factors along with political and economic conditions that shaped the course of history in this period [26].

While some consensus is forming around the concept of the LALIA, its exact timing and spatial extent are still debated [27,28]. The declining quality and quantity of annually resolved and absolutely dated climate proxy archives before medieval times [29,30], and the biological memory in tree-ring width measurements (that usually also reflect average growing season conditions rather than sub-seasonal extremes) [31] compromises proxy-model comparisons [32–35]. This has implications for our understanding of the relative contributions of external climate forcing versus internal climate dynamics [36,37], and for cross-disciplinary investigations into the entanglements of past climate variability and changes in human society (including the devastating ecological, agricultural, and societal effects of ephemeral cold spells) [38–40].

In seeking to provide a nuanced picture of the spatial and temporal characteristics of the onset of the LALIA, we present here more than one hundred double-stained wood anatomical thin sections from temperature-sensitive forest trees that grew in five continents between 530 and 550 CE. We focus the microscopic assessment of our global network on the identification and interpretation of three different types of precisely dated cell-level responses to distinct cold spells: Blue Rings (BRs), Frost Rings (FRs) and Light Rings (LRs) [41–50]. BRs signify reduced cell wall lignification, whereas FRs contain deformed and/or collapsed cells that may occur at any point in time during the growth period, and LRs refer to unusually thin cell walls in the latewood zone. All three anatomical features have been considered to reflect short-term, sub-seasonal cold spells rather than average growing season conditions that are usually captured by more traditional dendrochronological measurements, such as ring width and wood density. Finally, we describe intra- and interannual, as well as regional to large-scale patterns in the occurrence of anatomical responses and discuss their potential climatological implications in the context of the coldest episode of the past two millennia, the onset of LALIA.

2. Materials and methods

We compiled 106 absolutely dated wood samples from living and relict trees that grew at 23 high-elevation and high-latitude sites in both hemispheres (Fig. 2a). Each sample continuously covers the period 530–550 CE. The annual dating precision of most of the 23 tree-ring chronologies has been confirmed independently by the detection of globally coherent cosmogenic radiocarbon spikes in 774 and/or 993 CE [51]. Including 20 different species from ten genera and ranging from 1–16 trees per site (Table 1), our network spans an elevational gradient from near sea level in Alaska, Northern Ireland, Siberia, and New Zealand to 3870 m asl on the Tibetan Plateau in China (Table 1 and Fig. 2a). The dataset not only contains a wide range of biogeographic settings from temperate and boreal forest regions, but also represents different wood anatomical traits (Supplementary materials online) [52–54]. After cross-dating and quality control of each radial stem piece, rice starch was used to stabilise cell walls before thin sections were cut with a WSL-lab microtome [55]. The resulting ~15 µm thin sections were bleached with sodium/potassium hypochlorite to decolour cell walls and remove undesired cell content. A 1:4 blend of Safranin and Astra Blue was then used to stain lignified cell walls red and less-lignified cell walls blue [47]. The resulting 106 double-stained thin sections were repeatedly rinsed with water and ethanol at increasing concentrations, and finally embedded in glycerol under cover glasses. A high-magnification compound microscope was used to record the occurrence of BRs, FRs, and LRs (Fig. 2b), and produce high-resolution images (Figs. S1–S3 online). Ring widths between 530 and 550 CE were then measured on the same thin sections (Figs. S4 and S5, and Table S1 online).

3. Results

A total of 108 wood anatomical responses to abrupt cold spells are found in 20 out of 21 years between 530 and 550 CE, at 15 out of 17 high-elevation or high-latitude sites in the Northern Hemisphere (Table 1). The only year in which no cell-level anomaly was found is 547 CE. Moreover, BRs, FRs and LRs are entirely missing at two maritime sites in Alaska and Northern

Ireland (S1 and S11). Notably, no sign of ephemeral cooling is detected in any of the six sites and five species from the Southern Hemisphere. Followed by one LR in 530 CE in north-eastern Siberia (S17) and one BR in 531 CE in north-western Siberia (S15), three high-elevation sites in the western USA (S4–S6) reveal the first sign of an abrupt regional summer cooling event in 532 CE (Fig. 3a). Between one and two LRs are found in 533, 534, and 535 CE in north-eastern Siberia (S17) and the Altai Mountains (S18). Five out of seven sites in North America (S2–S6), two out of four sites in Europe (S12 and S14), and five out of six sites in Siberia and inner Eurasia (S16–S19) exhibit BRs in 536 CE (Figs. 3a, b and 4). In the same year, two and eight sites in the Northern Hemisphere contain FRs and LRs, respectively. Two sites in the western USA (S7) and north-western Siberia (S15) that did not show a BR in 536 CE exhibit a BR the year after, together with another two FRs and six LRs in 537 CE in North America and Eurasia. One BR (S12) and three LRs (S14, S15, and S17) are found in Europe and Siberia in 538 CE, and one BR (S16) and two LRs (S17 and S18) are found in Siberia in 539 CE. Dominated by sites in North America (S2–S7), the next cluster of four and six BRs is centred on 540 and 541 CE (Figs. 3a and 4), and supplemented by a total of five LRs in these consecutive years. One BR and FR each, and two LRs are found in 542 CE, followed by three BRs (S5, S15, and S20) and two LRs (S15 and S17) in 543 CE. Another cluster of three BRs and three LRs in North America and Eurasia dates to 548 CE (Figs. 3a and 4).

The overall lack of wood anatomical responses in Southern Hemisphere trees is remarkable because these species have been reported to exhibit BRs, FRs, and LRs in response to ephemeral cold spells (see Supplementary materials online). Our sub-seasonal resolved, wood anatomical evidence is consistent with the mean growing season ring width in the corresponding tree-ring chronologies (Fig. 3b), which suggest the strongest growth depressions across the Northern Hemisphere occurred in 536 and between 542 and 546 CE. Reflecting boreal summer conditions, the 17 individual site chronologies from North America and Eurasia exhibit exceptional year-to-year and decadal coherency, with a grand average inter-series correlation of 0.4 between 530 and 550 CE (Figs. S4 and S5 online). However, the tree-ring width chronologies from the Southern Hemisphere

have no variance in common. The most distinct growth suppressions in the Southern Hemisphere are related to the seasonal means between September and March in 532/3, 540/1, and 547/8 CE (Fig. 3b and Fig. S5b online).

The intra-annual timing of the three anatomical responses suggests a Northern Hemisphere-wide cold spell in 536 CE that likely peaked between mid-July and early-August (Fig. 5 and Figs. S1–S3 online). In the summer of 536 CE, 14 sites exhibit a total of 22 anatomical responses to cold. In 537 CE seven sites exhibit ten anatomical responses to cold. In both 540 and 541 CE six sites exhibit seven anatomical responses to cold, and in 548 CE five sites exhibit six anatomical responses to cold. Over the entire 21 years analysed between 530 and 550 CE, the Northern Quebec site (S3) and the Indigirka site (S17) contain the highest number of anatomical responses (Table 1 and Fig. 5), followed by sites in Alaska and Arizona (S2 and S6), the Italian Alps (S14), Yamal (S15) and the Altai (S18). A closer look into the species- and site-specific characteristics of the observed 89 BRs suggests that all of them were probably triggered by short cold spells at the end of growing season when the formation of tracheids was terminated, and the cambium was inactive (as previously described [47]). Similarly, all 93 LRs refer to the end of the growing season, and all FRs occurred well into the boreal growing season, after the formation of earlywood tracheids. Referring to different intensity levels of cell deformation and collapse, the nine FRs are characterised by banded rays, callus cells, and non-lignified tracheids (see Supplementary materials online for species-specific wood anatomical descriptions).

4. Discussion and conclusions

Using cell-level information from 106 trees in both hemispheres, this study represents the first large-scale wood anatomical perspective on the spatiotemporal occurrence of ephemeral cold spells in the mid-6th century. Our sub-seasonal insights into the onset of the LALIA between 530 and 550 CE are usually not offered by more traditional dendrochronological parameters (Fig. 1a, b), which are known to integrate longer growing season conditions between spring and autumn [5–7], and often

contain biological memory that damps interannual variability [31]. Although wood formation of all 20 species used here is largely sensitive to changes in growing season temperature (Figs. S1–S3 online), ring porous oak samples from Northern Ireland were not found to exhibit any BR. However, material from this site was included in our study because it had provided the first dendrochronological evidence for distinct summer cooling in 536 CE [19], which was described as a widespread dust-veil event associated with one or several large volcanic eruptions. This pioneering study also engaged with archaeological and historical records and set an agenda for the ice core community [2,8–10,56]. Independent dendrochronological and wood anatomical signs of the cold spell in 536 CE were later reported from high-elevation *Pinus* sp sites in the western USA [45,50], and from high-elevation or high-latitude *Larix* sp and *Pinus* sp sites in the Austrian Alps, the Russian Altai, Mongolia, northern Scandinavia, and Siberia [5,6,57–59].

With a total of 108 anatomical responses in 20 years at 15 extra-tropical sites in the Northern Hemisphere (Table 1), widespread evidence for ephemeral cooling during the boreal growing seasons of 536–537, 540–543, and 548 CE not only exceeds the sporadic background noise of BR and LR occurrence of up to two cases per year (Fig. 3a), but also coincides with the timing of sulfur fallout recorded in ice cores (Fig. 1d). Notably, FRs occur only in 536, 537, and 542 CE in the western USA, northern Scandinavia, and Mongolia (Figs. 2 and 3). The frequency and intensity of the observed anatomical responses to cold extremes at the onset of the LALIA appears particularly high when contrasted against the 378 individual tree rings from the Southern Hemisphere that do not exhibit a single sign. The distinct wood anatomical signatures for repeated Northern Hemisphere cold spells are somewhat reflected in the corresponding tree-ring width series (Fig. 3c and Fig. S5 online). The only year that is equally strongly captured by our wood anatomical and dendrochronological data is 536 CE.

The geographical patterns of the three major cold spells across the Northern Hemisphere extra-tropics reveal the widespread nature of the 536-event (Fig. 4), which seems to prolong into 537 CE mainly at two sites in the western USA (S7) and north-western Siberia (S15) where BRs were not

found in 536 CE. Comparison of the bi-annual patterns of 536/7 and 540/1 CE hint that the first event occurred slightly earlier in the growing season or was shorter (between mid-July and early-August), whereas cooling of the second event prolonged further into the succeeding year (or at least its effect on cell wall lignification). The intra-annual timing of the volcanic-induced radiative forcing and subsequent cooling in 536 CE could be associated with ancient eyewitness records of a solar dimming [5,17,19].

Although the spruce and larch sites in north-eastern Canada (S3) and north-eastern Siberia (S17) exhibit the highest number of anatomical responses to severe ephemeral cooling in 536/7, 540/1, and 548 CE (Figs. 3–5), their remote locations do not allow for any straightforward comparison with archaeological or historical records from the same regions. Nevertheless, we consider our findings a useful groundwork for deeper and more chronologically precise investigations into the volcano-climate-human nexus. For instance, the absence of wood anatomical responses at all six sites in the Southern Hemisphere (S8–S10 and S21–S23) suggests the LALIA was not a global event and its onset was possibly triggered by large volcanic eruptions in the Northern Hemisphere extra-tropics. Our findings further imply that the repeated regional- to large-scale cold spells between 532 and 548 CE were possibly mitigated by the vast oceans of the Southern Hemisphere. In this regard, we note also the lack of cooling signs at two maritime Northern Hemisphere sites in Alaska (S1) and Northern Ireland (S11). It could also be that rapid cooling occurred outside the austral growing season. In any case, the absence of anatomical responses in South America and Australasia is consistent with a generally muted signal of volcanic forcing in the Southern Hemisphere [60,61], which implies conceptual and methodological challenges of global climate averages.

The compilation of well-preserved and absolutely dated wood samples from the first half of the Common Era is challenged by a general lack of data prior to medieval times and inadequate archiving of relevant material that often originates from field campaigns conducted decades ago, with important metadata since lost [40]. With only six sites distributed across Chile, Argentina, Tasmania, and New Zealand, and no samples from Africa, our network is clearly biased towards the

Northern Hemisphere extra-tropics (Fig. 2a). It should be further noted that site-specific sample size ranges from 1–16 trees, with a mean of 4.6 wood pieces from any given location (Table 1). In addition to the network's geographical bias and inequality in sample replication, our site- and species-specific estimates of growing season lengths, which may range from a several weeks to almost half a year (Fig. 5), must be considered with caution. With approximately six weeks from mid-June to the end of July on the Taimyr Peninsula in northern Siberia (S16), and with up to six months from May to October in Northern Ireland (S11), the individual growing seasons not only vary substantially, but can also change from year-to-year by several days to weeks [62]. The relative early endings of xylogenesis at high-elevations in the western USA and high-latitudes in northern Siberia may partly explain why BRs at two sites were not formed in 536 CE but a year later (S7 and S15).

Moreover, the timing, intensity and duration of cold spells needed to trigger BR formation remain unclear [46–50], because of the yet unknown proportion of cell wall lignin, cellulose and other polysaccharides that are likely also affected by thermal conditions [63]. Although the concept of a cold threshold regulating biosynthesis of plant cell wall cellulose and hemicellulose is generally known, the biotic and abiotic drivers of lignin formation remain uncertain. Moreover, the eco-physiological and biochemical factors and processes relevant for plant cell wall lignification are highly complex and still under debate [64]. Future research should therefore explore the thermal limits of biosynthesis within different cell wall components to unravel the factors responsible for xylogenesis and lignin formation. Performed either under controlled laboratory or open field experiments, such studies should consider plant stem anatomical analyses of different cell functional types across the largest trees and smallest herbs to quantify the climatic controls of BRs within and between species and lifeforms. For example, mutants of the model plant *Arabidopsis thaliana* (L.) Heynh with and without the expression of lignin-relevant key enzymes could be used to investigate the biochemical basis for a putative temperature threshold for lignin formation [65], and to explore the ability of lignin to penetrate cell walls. Genetic control of different types of lignin in plant cell

walls is expected to provide new insights into the potential and limitations of Safranin and Astra Blue double-staining. A confocal fluorescence imaging approach, applied to samples stained only with Safranin, is likely to enable quantitative assessments of cell wall lignification in BRs [66]. This could reveal variance in the level of cell wall lignin between different BRs, which may infer further climatic information beyond what is currently possible from the rather simplified binary BR classification used here and in most prior studies.

In conclusion, our study demonstrates the advantage of well-replicated wood anatomical investigations over traditional tree-ring measurements (i.e., ephemeral shocks versus growing season integrals), and emphasizes the importance of double-stained thin sections that reveal biochemical responses beyond anatomical anomalies (i.e., BRs versus FRs and LRs). The improved archive resolution of our wood anatomical network will hopefully open new pathways for cross-disciplinary investigations into the direct and indirect relationships between volcanic eruptions, climatic changes, and ecological and societal responses at sub-seasonal timescales.

Conflict of interest

The authors declare that they have no conflict of interest.

Acknowledgments

Ulf Büntgen and Jan Esper received funding from the ERC Advanced Project MONOSTAR (AdG 882727). Ulf Büntgen, Jan Esper, and Mirek Trnka received funding from SustES: adaptation strategies for sustainable ecosystem services and food security under adverse environmental conditions (CZ.02.1.01/0.0/0.0/16_019/0000797). Ulf Büntgen, Jan Esper, and Clive Oppenheimer discussed many aspects of this study at the Center for Interdisciplinary Research (ZiF) at the University of Bielefeld, Germany. Alan Crivellaro received funding from the Fritz & Elisabeth Schweingruber Foundation. Duncan A. Christie and Carlos Le Quesne received funding from the ANID (FONDECYT 1201411, 1221307, FONDAP 15110009, BASAL FB210018). Olga V.

Churakova (Sidorova) received funding from the Russian Science Foundation grant (RSF 21-17-00006). Rosanne D'Arrigo received funding from NSF Arctic Social Science 2112314 and NSF Arctic Natural Science 2124885, as well as the NSF P2C2 (Paleo Perspectives on Climatic Change) program (various grants). Rashit M. Hantemirov received funding from the Russian Science Foundation grant (RSF 21-14-00330). Alexander V. Kirdyanov received funding from the Russian Science Foundation grant (RSF 18-14-00072P). Fredrik C. Ljungqvist was supported by the Swedish Research Council (2018-01272). Patrick Fonti and Markus Stoffel received funding from the Swiss National Science Foundation through the SNSF Sinergia CALDERA project (CRSII5 183571). Matthew Salzer and Malcolm K. Hughes received funding from The National Science Foundation's P2C2 program (1902625 and 1203749) and from the Malcolm H. Wiener Foundation. Greg Wiles was funded through NSF P2C2 program (2002454).

Author contributions

Ulf Büntgen designed the study and wrote the first draft of this manuscript with input from Jan Esper, Paul J. Krusic, and Clive Oppenheimer. Samples were processed and analysed by Alma Piermattei and Alan Crivellaro. All authors provided data and/or contributed to discussion and improving the article.

References

[1] Stothers RB. Mystery cloud of AD 536. Nature 1984;307:344–345.

[2] Sigl M, Winstrup M, McConnell JR, et al., Timing and climate forcing of volcanic eruptions for the past 2500 years. Nature 2015;523:543–549.

[3] Dull RA, Southon JR, Kutterolf S, et al. Radiocarbon and geologic evidence reveal Ilopango volcano as source of the colossal 'mystery' eruption of 539/40 CE. Quat Sci Res 2019;222:105855.

[4] Sinitul VC, Costa A, Aguirre-Díaz G, et al. The magnitude and impact of the 431 CE Tierra Blanca Joven eruption of Ilopango, El Salvador. Proc Nat Aca Sci USA 2020;117:26061–26068.

[5] Büntgen U, Myglan VS, Ljungqvist FC, et al. Cooling and societal change during the Late Antique Little Ice Age from 536 to around 660 AD. Nat. Geosci 2016;9:231–236.

[6] Büntgen U, Arseneault D, Boucher É, et al. Prominent role of volcanism in Common Era climate variability and human history. Dendrochronologia 2020;64:125757.

[7] Büntgen U, Allen K, Anchukaitis K, et al. The influence of decision-making in tree ring-based climate reconstructions. Nat Commun 2021;12:3411.

[8] Toohey M, Krüger K, Sigl M, et al. Climatic and societal impacts of a volcanic double event at the dawn of the Middle Ages. Clim Change 2016;136:401–412.

[9] Sigl M, Toohey M, McConnell JR, et al. Volcanic stratospheric sulfur injections and aerosol optical depth during the Holocene (past 11,500 years) from a bipolar ice core array. Earth Syst Sci Data 2022;14:3167–3196.

[10] Toohey M, Sigl M. Volcanic stratospheric sulfur injections and aerosol optical depth from 500 BCE to 1900 CE. Earth Syst Sci Data 2017;9:809–831.

[11] Mason OK, Jensen AM, Rinck B, et al. Heightened early medieval storminess across the Chukchi Sea, AD 400–1100: a proxy of the Late Antique Little Ice Age. Quat Int 2020;549:98–117.

[12] Oinonen M, Alenius T, Arppe L, et al. Buried in water, burdened by nature—Resilience carried the Iron Age people through Fimbulvinter. PLoS One 2020;15:e0231787.

[13] Peregrine PN. Climate and social change at the start of the Late Antique Little Ice Age. Holocene 2020;30:1643–1648.

[14] Pilø L, Finstad E, Barrett JH. Crossing the ice: an Iron Age to medieval mountain pass at Lendbreen, Norway. Antiquity 2020;94:437–454.

[15] Bajard M, Bard E, Høeg HI, et al. Climate adaptation of pre-Viking societies. Quat Sc Rev 2022;278:107374.

[16] Moreland J. AD 536—Back to Nature? Acta Archaeol 2018;89:91–111.

[17] Newfield TP. The Climate Downturn of 536-50. In: White S, Pfister C, Mauelshagen F, eds. The Palgrave handbook of climate history. Berlin: Springer 2018;1:447–493.

[18] Bar-Oz G, Weissbrod L, Erickson-Gini T, et al. Ancient trash mounds unravel urban collapse a century before the end of Byzantine hegemony in the southern Levant. Proc Nat Aca Sci USA 2019;116:8239–8248.

[19] Baillie MGL. Dendrochronology raises questions about the nature of the AD 536 dust veil event. Holocene 1994;4:212– 217.

[20] Arjava A. The mystery cloud of 536 CE in the Mediterranean sources. Dumbart. Oaks Pap 2005;59:73e94.

[21] Harper K. The fate of Rome: climate, disease, and the end of an empire. Princeton: Princeton University Press, 2017.

[22] Keys D. Catastrophe: an investigation into the origins of the modern world. New York: Ballantine Books, 2000.

[23] Oppenheimer C. Eruptions that shook the world. Cambridge: Cambridge University Press 2011.

[24] Workman WB, Workman K W. The end of the Kachemak tradition on the Kenai Peninsula, southcentral Alaska. Arctic Anthropol 2010;47:90–96.

[25] Gräslund B, Price N. Twilight of the gods? The ‘dust veil event’ of AD 536 in critical perspective. Antiquity 2012;86:428–443.

[26] Haldon J. Cooling and societal change. Nat Geosci 2016;9:191–192.

[27] Helama S, Jones PD, Briffa KR. Limited Late Antique cooling. Nat Geosci 2017;10:242–243.

[28] Büntgen U, Myglan VS, Ljungqvist FC, et al. Reply to ‘Limited Late Antique cooling’. Nat Geosci 2017;10:243.

[29] Esper J, Büntgen U. The future of paleoclimate. Clim Res 2021;83:57–59.

[30] Anchukaitis KJ, Smerdon JE. Progress and uncertainties in global and hemispheric temperature reconstructions of the Common Era. Quat Sci Rev 2022;286:107537.

[31] Esper J, Schneider L, Smerdon J, et al. Signals and memory in tree-ring width and density data. Dendrochronologia 2015;35:62–70.

[32] Anchukaitis KJ, Breitenmoser P, Briffa KR, et al. No evidence for misdating of tree-ring chronologies associated with volcanic cooling. Nat Geosci 2012;5:836–837.

[33] Esper J, Büntgen U, Hartl-Meier CTM, et al. Northern Hemisphere temperature anomalies during the 1450s period of ambiguous volcanic forcing. Bull Volcanol 2017;79:41.

[34] Hartl-Meier CTM, Büntgen U, Smerdon JE, et al. Temperature covariance in tree-ring reconstructions and climate model simulations over the past millennium. Geophys Res Lett 2017;44:9458–9469.

[35] Ljungqvist FC, Zhang Q, Brattström G, et al. Centennial-scale temperature change in last millennium simulations and proxy-based reconstructions. J Clim 2019;32:2441–2482.

[36] Kelley C, Ting M, Seager R, et al. The relative contributions of radiative forcing and internal climate variability to the late 20th Century winter drying of the Mediterranean region. Clim Dyn 2012;38:2001–2015.

[37] Boeke RC, Taylor PC. Seasonal energy exchange in sea ice retreat regions contributes to differences in projected Arctic warming. Nat Commun 2018;9:5017.

[38] Degroot D, Anchukaitis K, Bauch M, et al. Towards a rigorous understanding of societal responses to climate change. Nature 2021;591:539–550.

[39] Ljungqvist F, Seim A, Huhtamaa H. Climate and society in European history. Wiley Interdiscip Rev Clim Chang 2021;12:2691.

[40] Büntgen U, Esper J, Oppenheimer C. In praise of archives (and an open mind). Commun Earth Environ 2022;3:84.

[41] LaMarche VC, Hirschboeck K. Frost rings in trees as records of major volcanic eruptions. Nature 1984;307:121–126.

[42] Filion L, Payette S, Boutin Y. Light rings in subarctic conifers as a dendrochronological tool. Quat Res 1986;26:272–279.

[43] Burnstein FC. Latewood frost-ring record at Almagre Mountain, Colorado, U.S.A. Arctic Alpine Res 1996;28:65–76.

[44] Wang L, Payette S, Bégin Y. A quantitative definition of Light Rings in Black Spruce (*Picea mariana*) at the Arctic treeline in Northern Québec, Canada. Arctic, Antarctic Alpine Res 2000;32:324–330.

[45] Salzer MW, Hughes MK. Bristlecone pine trees and volcanic eruptions over the last 5000 yr. Quat Res 2007;67:57e68.

[46] Piermattei A, Crivellaro A, Carrer M, et al. The 'blue ring': anatomy and formation hypothesis of a new tree-ring anomaly in conifers. Trees 2015;29:613–20.

[47] Piermattei A, Crivellaro A, Krusic PJ, et al. A millennium-long 'Blue-Ring' chronology from the Spanish Pyrenees reveals sever ephemeral summer cooling after volcanic eruptions. Environ Res Lett 2020;15:124016.

[48] Crivellaro A, Reverenna M, Ruffinatto F, et al. The anatomy of blue ring in the wood of *Pinus nigra*. Les/Wood 2018;67:21–28.

[49] Crivellaro A, Büntgen U. New evidence of thermally-constraint plant cell wall lignification. Trends Plant Sci 2020;24:322–324.

[50] Tardif JC, Salzer MW, Conciatori F, et al. Formation, structure and climatic significance of blue rings and frost rings in high elevation bristlecone pine (*Pinus longaeva* D.K. Bailey). Quat Sci Rev 2020;244:106516.

[51] Büntgen U, Wacker L, Galván JD, et al. Tree rings reveal globally coherent signature of cosmogenic radiocarbon events in 774 and 993 CE. Nat Commun 2018;9:3605.

[52] Roig FA. Comparative wood anatomy of southern South American Cupressaceae. IAWA J 1992;13:151–162.

[53] Crivellaro A, Schweingruber F. Stem anatomical features of dicotyledons. Norbert: Kessel 2015.

[54] Ruffinatto F, Crivellaro A. Atlas of macroscopic wood identification: with a special focus on timbers used in Europe and CITES-listed species. Berlin: Springer, 2019.

[55] Gärtner H, Cherubini P, Fonti P, et al. Technical challenges in tree-ring research including wood anatomy and dendroecology. J Visual Exp 2015;97:e52337.

[56] Larsen LB, Vinther BM, Briffa KR, et al. New ice core evidence for a volcanic cause of the A.D. 536 dust veil. Geophys Res Lett 2008;35:L04708.

[57] D'Arrigo R, Frank D, Jacoby G, et al. Spatial response to major volcanic events in or about AD 536, 934 and 1258: frost rings and other dendrochronological evidence from Mongolia and northern Siberia: comment on RB Stothers "Volcanic dry fogs, climate cooling, and plague pandemics in Europe and the Middle East". Clim Change 2001;49:239–246.

[58] Churakova (Sidorova) OV, Bryukhanova MV, Saurer M, et al. A cluster of stratospheric volcanic eruptions in the AD 530s recorded in Siberian tree rings. Glob Plan Change 2014;122:140–150.

[59] Helama S, Saranpää P, Pearson CL, et al. Frost rings in 1627 BC and AD 536 in subfossil pinewood from Finnish Lapland. Quat Sci Rev 2019;204:208–215.

[60] Büntgen U, Smith S H, Wagner S, et al. Global tree-ring response and inferred climate variation following the mid-thirteenth century Samalas eruption. Clim Dyn 2022;59:531–546.

[61] Higgins PA, Palmer JG, Turney CSM, et al. Do Southern Hemisphere tree rings record past volcanic events? A case study from New Zealand. Clim Past 2022;18:1169–1188.

[62] Büntgen U, Piermattei A, Krusic PJ, et al. Plants in the UK flower a month earlier under recent warming. Proc R Soc B Biol Sci 2022;289:20212456.

[63] Begum S, Nakaba S, Yamagishi Y, et al. Regulation of cambial activity in relation to environmental conditions: understanding the role of temperature in wood formation of trees. Physiol Planta 2013;147:46–54.

[64] Kumar M, Campbell L, Turner S. Secondary cell walls: biosynthesis and manipulation. J Exp Bot 2016;67:515–531.

[65] Sardans J, Gargallo-Garriga A, Urban O, et al. Ecometabolomics for a better understanding of plant responses and acclimation to abiotic factors linked to global change. Metabolites 2020;10:239.

[66] Baldacci-Cresp F, Spriet C, Twyffels L, et al. A rapid and quantitative safranin-based fluorescent microscopy method to evaluate cell wall lignification. Pant J 2020;102:1074–1089.

Table 1. Network characteristics[a)]

Code	Site	Latitude	Longitude	Elevation (m asl)	Main species	Samples	Blue Rings	Frost Rings	Light Rings
S1	Tebenkof Glacier, USA	60.75°N	148.50°W	50	*Tsuga mertensiana*	4	0	0	0
S2	Glacier Bay, USA	58.60°N	136.55°W	500	*Picea stichensis*	16	5 (1.5%)	0	1 (0.3%)
S3	Northern Quebec, Canada	54.60°N	70.30°W	580	*Picea mariana*	4	10 (11.9%)	0	10 (11.9%)
S4	Mt Washington, USA	38.90°N	114.30°W	3400	*Pinus longaeva*	8	16 (9.5%)	0	0
S5	Sheep Mt, USA	37.55°N	118.20°W	3500	*Pinus longaeva*	4	7 (8.3%)	0	0
S6	San Francisco Peaks, USA	35.30°N	111.65°W	3530	*Pinus aristata*	4	9 (10.7%)	2 (2.4%)	0
S7	Chicken Spring Lake, USA	34.45°N	118.20°W	3450	*Pinus balfouriana*	2	3 (7.1%)	0	0
S8	El Asiento, Chile	32.65°S	70.80°W	1940	*Austrocedrus chilensis*	2	0	0	0
S9	El Cepillo, Chile	34.55°S	70.55°W	2000	*Austrocedrus chilensis*	2	0	0	0
S10	Rio Alerzal, Argentina	42.75°S	72.00°W	550	*Fitzroya cupressoides*	6	0	0	0
S11	Northern Ireland, UK	54.75°N	6.95°W	10	*Quercus sp*	5	0	0	0
S12	N Scandinavia, Finland	67.20°N	25.15°E	300	*Pinus sylvestris*	2	5 (11.9%)	1 (2.4%)	4 (7.1%)
S13	Austrian Alps, Austria	47.25°N	11.60°E	2050	*L. decidua, P. cembra*	2	0	0	1 (2.4%)
S14	Italian Alps, Italy	46.30°N	10.85°E	1950	*Larix decidua*	10	7 (3.3%)	0	11 (5.2%)
S15	Yamal, Russia	67.40°N	70.10°E	30	*Larix sibirica*	5	10 (9.5%)	0	15 (14.3%)
S16	Taimyr, Russia	72.50°N	102.60°E	10	*Larix gmelinii*	6	7 (5.6%)	0	10 (7.9%)
S17	Indigirka, Russia	65.30°N	143.15°E	400	*Larix cajanderi*	5	1 (1.0%)	1 (1.0%)	23 (21.9%)
S18	Altai, Russia	50.60°N	86.20°E	2200	*Larix sibirica*	9	4 (2.1%)	4 (44%)	19 (10.1%)
S19	Sol Dav, Mongolia	48.30°N	98.95°E	2420	*Pinus sibirica*	2	2 (4.8%)	1 (2.4%)	0
S20	Tibetan Plateau, China	37.30°N	97.45°E	3870	*Juniperus przewalskii*	1	3 (14.3%)	0	0
S21	Mt Read, Tasmania	41.80°S	145.40°E	570	*Lagarostrobos franklinii*	5	0	0	0
S22	North Kaipara, New Zealand	36.10°S	174.00°E	50	*Agathis australis*	1	0	0	0
S23	Oroko Swamp, New Zealand	43.25°S	170.30°E	120	*Manoao colensoi*	2	0	0	0

a) Name, location and elevation, main species, sample size, as well as the total number and percentage of detected Blue Rings (BRs), Frost Rings (FRs) and Light Rings (LRs) between 530 and

550 CE (inclusive) of each of the 23 sites in both hemispheres (S1–S23). Sites are ordered from north-west to south-east.

Fig. 1. Temperature variability and volcanic activity. (a) Ensemble of 15 slightly different Northern Hemisphere summer temperature reconstructions from 0–2016 CE [7], together with their mean and median (orange and red); (b) a closer look into temperature changes at the onset of the Late Antique Little Ice Age (LALIA) between 530 and 550 CE. (c) Estimated Northern Hemisphere extra-tropical Stratospheric Aerosol Optical Depth (SAOD) from 0–2016 CE [9], with the largest known volcanic eruptions named; (d) a closer look into cumulative volcanic sulphate flux between 530 and 550 CE [10], with the light brown bar referring to the Southern Hemisphere.

Fig. 2. Wood anatomical network. (a) Location of 23 sampling sites of 20 different species from ten genera in both hemispheres (see Table 1 for details), separated into 12 high-latitude, low-elevation sites <580 m asl and 11 mid-latitude, high-elevation sites between 1900 and 3870 m asl (triangles and circles), with symbol sizes referring to the number of samples ranging from 1–16 cores or discs per site. Map produced with QGIS and downloaded from Natural Earth (free vector and raster map data, natruralearthdata.com). (b) The three main wood anatomical responses to abrupt growing season cooling between spring and autumn: a Blue Ring (BR; lack of cell wall lignification), Frost Ring (FR; cell deformation) and Light Ring (LR; reduced cell wall thickening), formed in 536 CE (black dots) in larch (*Larix sibirica*), pine (*Pinus aristata*) and larch (*Larix sibirica*) trees in the Altai, Arizona, and Yamal (there is also a LR in 537 CE in the Yamal sample), respectively.

Fig. 3. Wood anatomical and dendrochronological responses. (a) Temporal distribution of Blue Rings (BRs), Frost Rings (FRs), and Light Rings (LRs) between 530 and 550 CE (see Table 1 and Fig. 1 for the individual site codes). (b) Double-stained *Pinus sylvestris* thin section from Northern Scandinavia (S12), which covers 530–550 CE and reveals a distinct BR in 536 CE. (c) Tree-ring

width (TRW) measurements averaged over 17 sites (84 trees) in the Northern Hemisphere (green line) and six sites (15 trees) in the Southern Hemisphere (orange line). The individual raw TRW series were normalized to have a mean of zero and a standard deviation of one over 530–550 CE (see Fig. S5 online for the individual site chronologies). Since the seasonal formation of secondary cell walls in the extra-tropics of the Southern Hemisphere starts in the boreal autumn of a given year and ends in the boreal spring of the following year, austral tree-ring series should lag rather than precede those from the Northern Hemisphere by approximately six months.

Fig. 4. Spatial wood anatomical responses. Spatial distribution of Blue Rings (BRs; dark blue fillings), Frost Rings (FRs; blue frames) and Light Rings (LRs; light blue vertical lines) in the most affected years between 536 and 548 CE across the Northern Hemisphere extra-tropics, where only two maritime sites in Alaska (S1; *Tsuga mertensiana*) and Northern Ireland (S11; *Quercus* sp) do not exhibit wood anatomical anomalies. Map produced with QGIS and downloaded from Natural Earth (free vector and raster map data, natruralearthdata.com).

Fig. 5. Intra-annual wood anatomical responses. Occurrence and timing of Blue Rings (BRs; dark blue frames), Frost Rings (FRs; blue frames) and Light Rings (LRs; light blue horizontal lines) within and between in the most affected years between 536 and 548 CE across the Northern Hemisphere extra-tropics, where only two maritime sites in Alaska (S1; *Tsuga mertensiana*) and Northern Ireland (S11; *Quercus* sp) do not exhibit wood anatomical anomalies. The green horizontal bars refer to the site- and species-specific individual growing season lengths (see Table S1 online for details), and superimposed are the estimated timings of BRs, FRs and LRs. Figures in italic at the top and bottom (and right) refer to the number of sites (or years) in which one or more anatomical responses were found and the total amount of anatomical responses per year (or per site).

Ulf Büntgen is a professor of environmental systems analysis at the Department of Geography, University of Cambridge, UK. He is also professor of physical geography at the Department of Geography, Masaryk University in Brno, Czech Republic, Research Associate at CzechGlobe, Global Change Research Institute of the Czech Academy of Science in Brno, Czech Republic, and Senior Scientist at the Swiss Federal Research Institute for Forest Snow and Landscape in Birmensdorf, Switzerland. He is a dendrochronologist, paleo-climatologist, and global change ecologist.

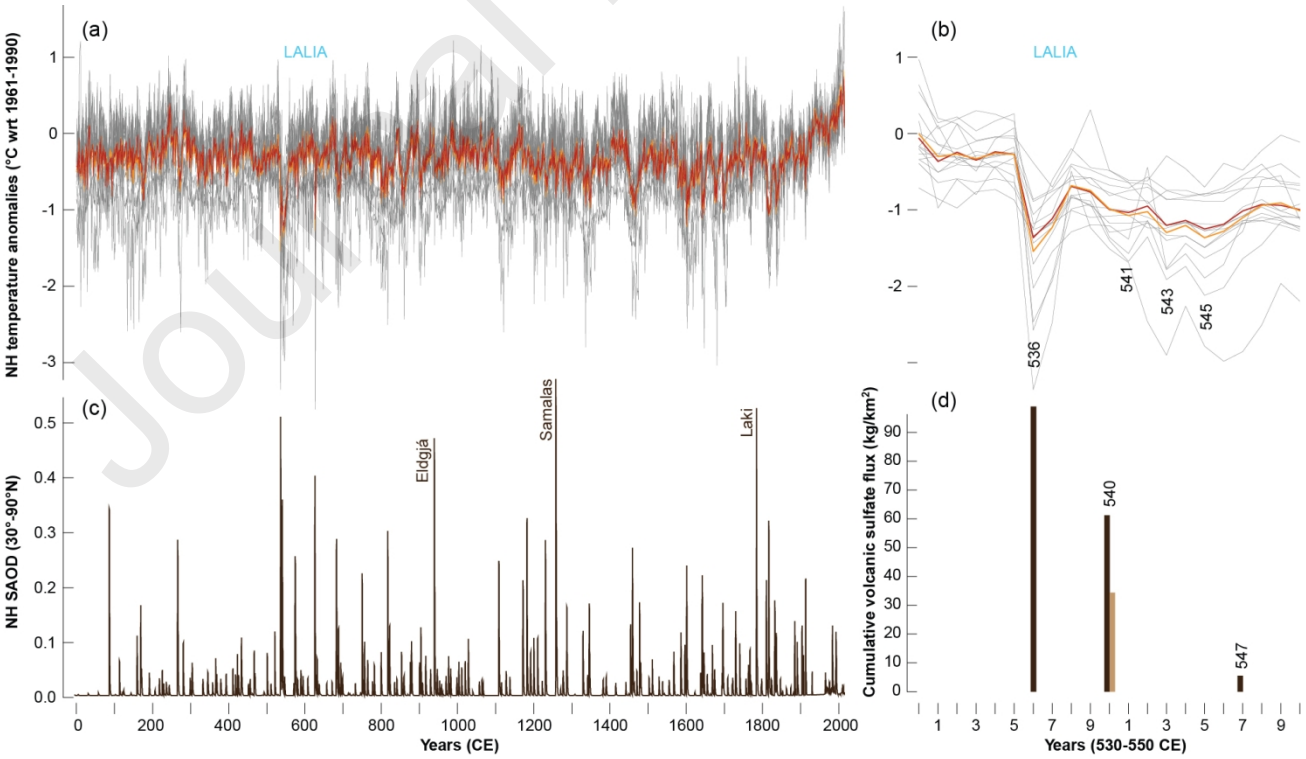

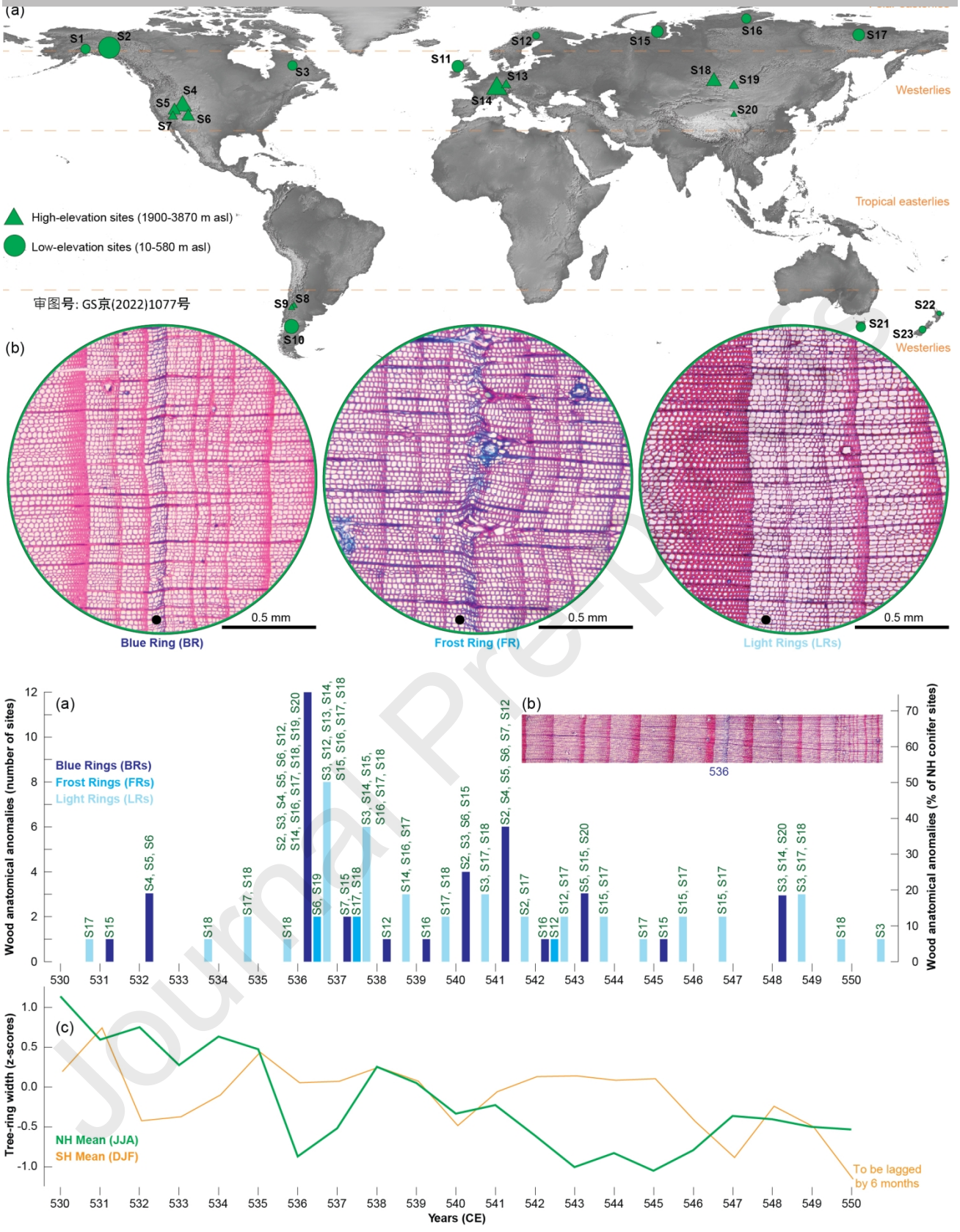

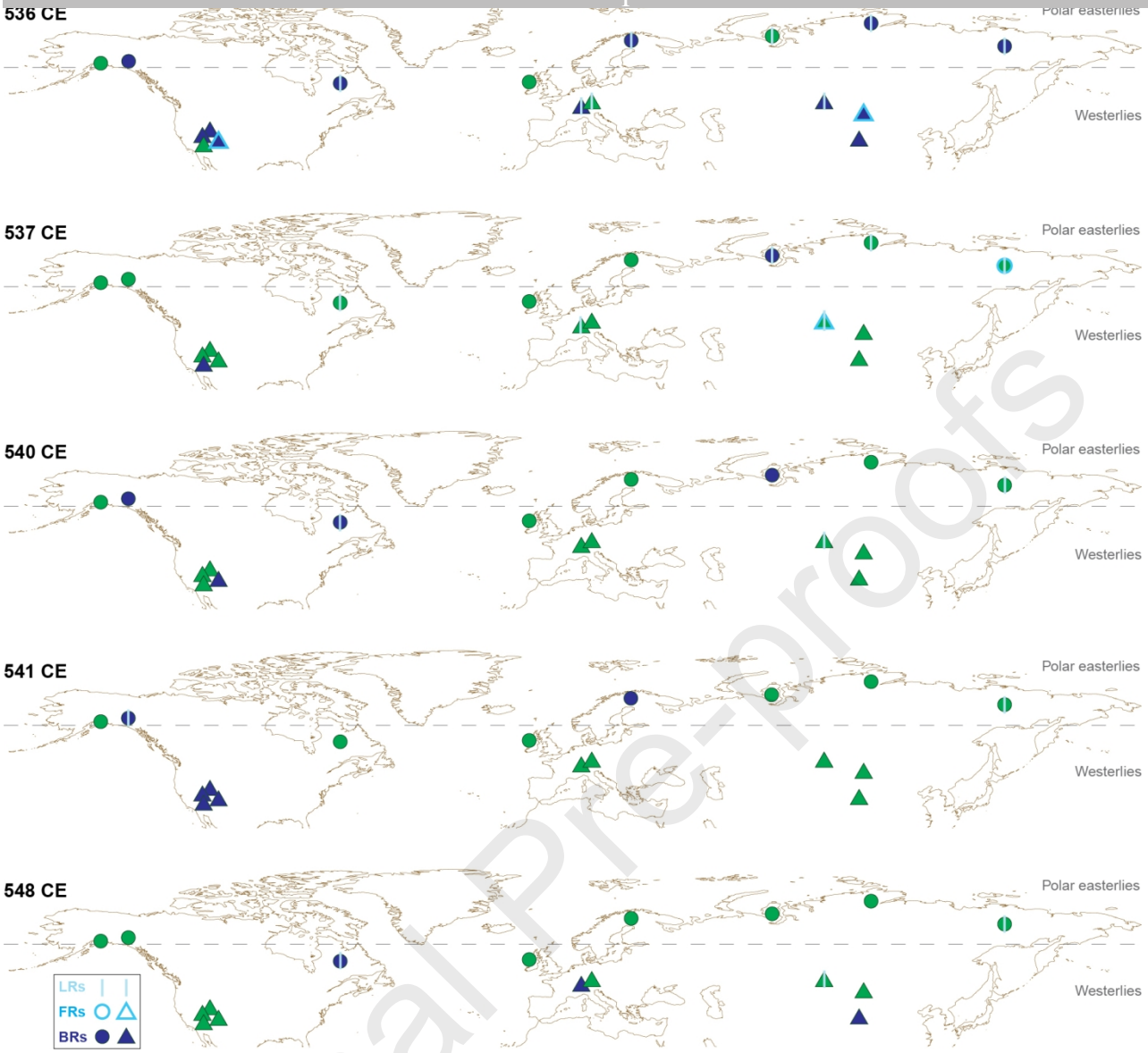

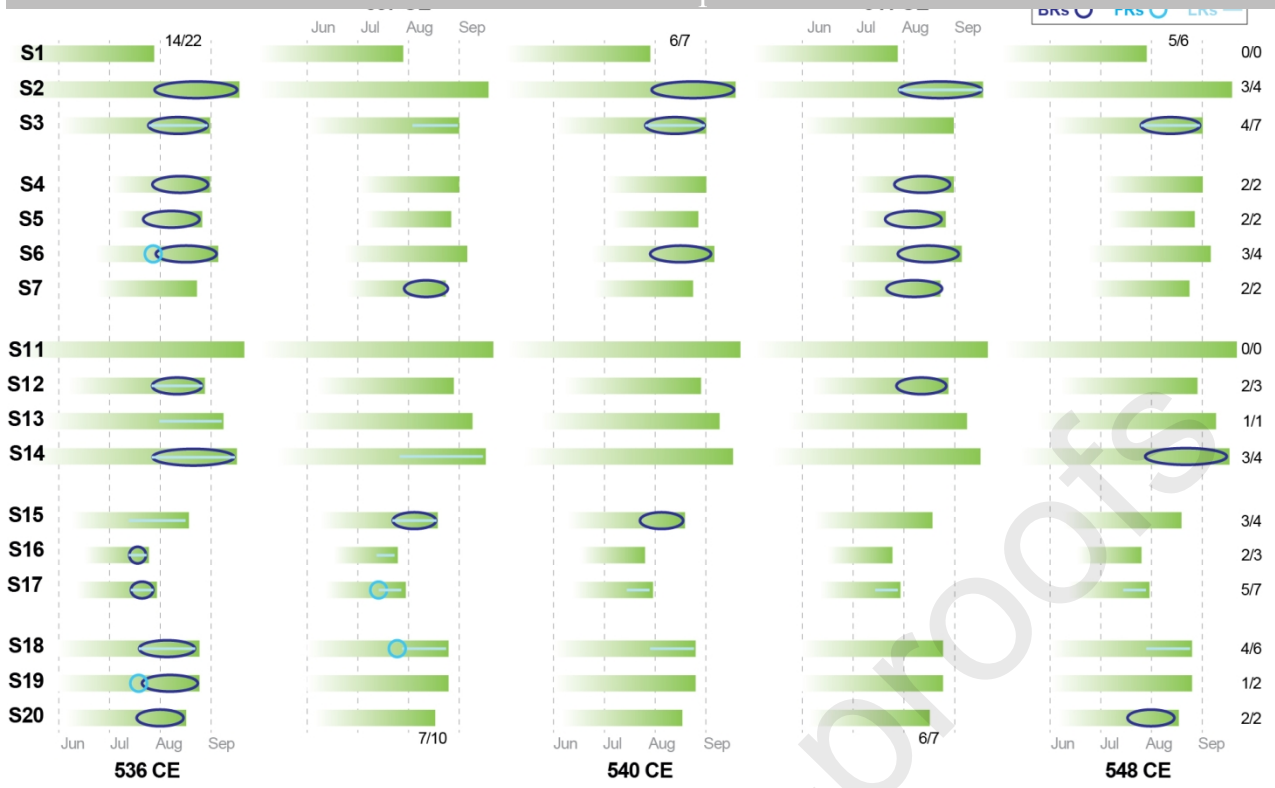

Graphical Abstract for:

Global wood-anatomical perspective on the onset of the Late Antique Little Ice Age (LALIA) in the mid-6th century CE

by Ulf Büntgen et al.

Graphical Abstract. (**a**) Ensemble of 15 slightly different Northern Hemisphere summer temperature reconstructions from 0–2016 CE, together with their mean and median (orange and red), and a closer look into temperature changes at the onset of the Late Antique Little Ice Age (LALIA) between 530 and 550 CE. (**b**) Location of 23 sampling sites of 20 different species from ten genera in both hemispheres (see Table 1 for details), separated into 12 high-latitude sites <580 m asl and 11 high-elevation sites between 1900 and 3800 m asl (triangles and circles), with individual symbol

sizes referring to 1–16 core or disc samples per site. (**c**) The three main wood anatomical responses to abrupt summer cooling: a Blue Ring (lack of cell wall lignification), Frost Ring (cell deformation) and Light Ring (reduced cell formation), formed in 536 CE by larch (*Larix sibirica*), pine (*Pinus balfouriana*) and larch (*Larix sibirica*) trees in the Altai, Arizona, and Yamal, respectively. (**d**) Temporal distribution of Blue Rings (BRs), Frost Rings (FRs) and Light Rings (LRs) between 530 and 550 CE.

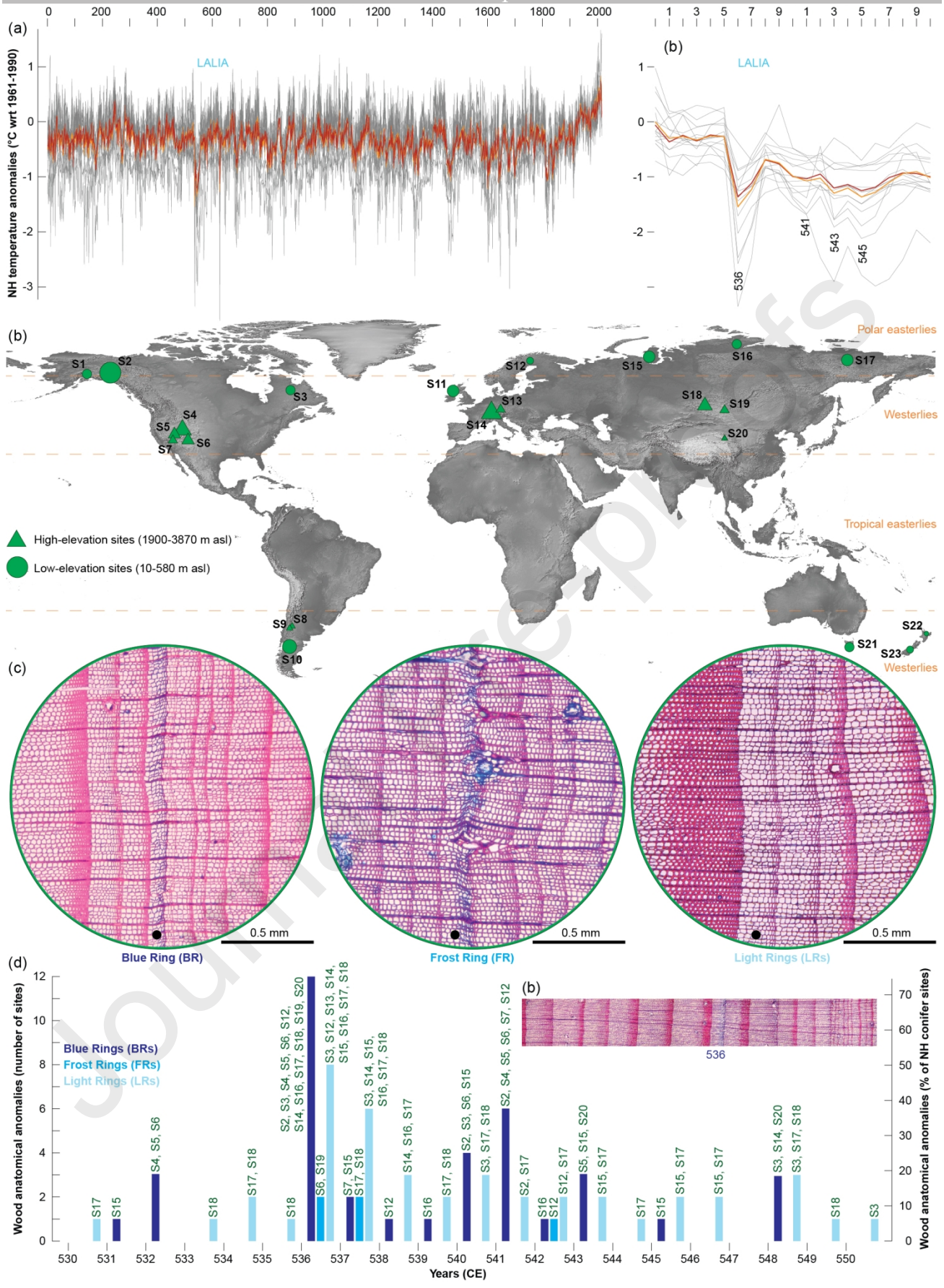
(a)
LALIA
NH temperature anomalies (°C wrt 1961-1990)
(b)
LALIA
536
541
543
545
(b)
Polar easterlies
Westerlies
Tropical easterlies
Westerlies
S1
S2
S3
S4
S5
S6
S7
S8
S9
S10
S11
S12
S13
S14
S15
S16
S17
S18
S19
S20
S21
S22
S23
High-elevation sites (1900-3870 m asl)
Low-elevation sites (10-580 m asl)
(c)
0.5 mm
Blue Ring (BR)
0.5 mm
Frost Ring (FR)
0.5 mm
Light Rings (LRs)
(d)
Wood anatomical anomalies (number of sites)
Blue Rings (BRs)
Frost Rings (FRs)
Light Rings (LRs)
Years (CE)
(b)
536
Wood anatomical anomalies (% of NH conifer sites)